Progress of Combustion Research by Large-scale Detailed Numerical Simulation(Mathematical Sciences for Large Scale Numerical Simulations)

AUTHOR(S):

Mizobuchi, Yasuhiro; Takeno, Tadao

数理解析研究所講究録
第 1573 巻 2007 年 63-72

Progress of Combustion Research by Large-scale Detailed Numerical Simulation

Yasuhiro Mizobuchi, Japan Aerospace Exploration Agency
Tadao Takeno, Meijo University

1. Introduction

The recent advancement in computer power and computational technique is remarkable, and it has brought a new scientific approach, numerical experiment, which has been proven successful in understanding the complicated phenomena such as turbulence and combustion. We can extract a lot of important information from the simulated data because we are supposed to be able to measure all the quantities considered at any point in space and time provided that the simulation properly reproduce the phenomena.

The size of detailed physics simulation used to be so small that the simulation looks like an imaginary world simulation, because the smallest scales, for example, the eddy size of turbulence and the reaction layer thickness of combustion, are extremely small, and therefore, quite large numbers of grid points are necessary to simulate real world problems. But thanks to the recent progress of computation ability, 'real-size' simulation is coming possible, here 'real-size' means 'possible to compare with real world experimental measurements'. As for the combustion simulation, the size is still small compared with the practical applications, but 3-D combustion simulations can be conducted about the laboratory-size flames with detailed physics.

Thanks to the development of optical technique, the non-intrusive measurement of combustion flow field is becoming possible. But most of the measurement is still 2-D and is not yet quantitative. The resolution is almost high enough to look at the envelope of the combustion field but not enough to investigate into the internal detailed structure. Hence, at this moment, numerical experiment is thought to be the only means to look into the 3-D complicated structure of combustion phenomena.

In series of studies of the authors, a hydrogen jet lifted flame has been successfully reproduced by a highly resolved large-scale numerical simulation with detailed chemistry and rigorous transport properties [1)-3)]. The analysis of the obtained data has revealed some interesting aspects of the flame. In this paper, we mainly try to identify the new findings observed throughout the study.

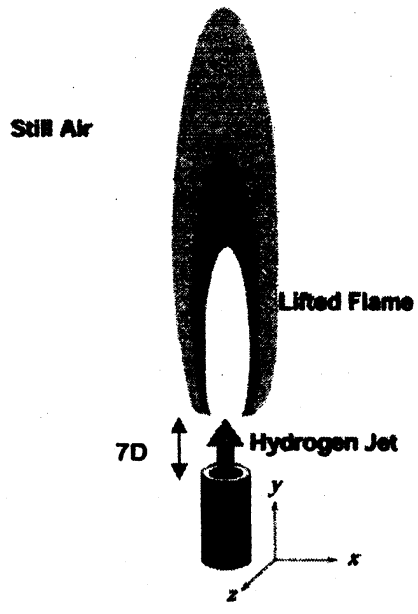

Figure 1: Hydrogen jet lifted flame

2. Flame configurations

The simulated flame is a jet lifted flame produced by combustion of a subsonic pure hydrogen jet injected from a round nozzle to still atmosphere. The jet velocity is 680m/sec and the nozzle diameter D is 2mm. The observed lift-off height is about 7D in the experiment by Cheng et al. [4].

3. Numerical Simulation

3.1. Numerical model and governing equations

The 9-species (H_2, O_2, OH, H_2O, H, O, H_2O_2, HO_2 ,N_2) and 17-reaction model [5] is used for the H_2/air reaction system. The elementary reactions are shown in Table 1. The transport coefficients are calculated rigorously using inter-molecular potential model[6,7]. The enthalpy of each chemical species is quoted from JANAF table[8].

The governing equations are the time-dependent 3-D Navier-Stokes equations coupled with the conservation equations of 9 chemical species. They are written in the generalized curvilinear coordinate system as,

$$\frac{\partial Q}{\partial \tau}+\frac{\partial F_{\xi_i}}{\partial \xi_i}=\frac{\partial F_{v\xi_i}}{\partial \xi_i}+H_c, \tag{1}$$

$$Q=V\begin{bmatrix}\rho\\ \rho u_1\\ \rho u_2\\ \rho u_3\\ E\\ \rho z_s\end{bmatrix},\quad F_{\xi_i}=\begin{bmatrix}n_{ij}\rho u_j\\ n_{ij}\rho u_1u_j+n_{i1}p\\ n_{ij}\rho u_2u_j+n_{i2}p\\ n_{ij}\rho u_3u_j+n_{i3}p\\ n_{ij}(E+p)u_j\\ n_{ij}\rho z_su_j\end{bmatrix},\quad F_{v\xi_i}=\begin{bmatrix}0\\ n_{ij}\tau_{1j}\\ n_{ij}\tau_{2j}\\ n_{ij}\tau_{3j}\\ n_{ij}\left(\tau_{jk}u_k+q_j\right)\\ n_{ij}\rho D_sz_{s,j}\end{bmatrix},$$

$$E=e+\frac{1}{2}\rho(u_1^2+u_2^2+u_3^2),$$
$$e=\sum_s \rho z_s(H_s+\Delta H_{fs})-p,$$
$$p=R_uT\sum_s \rho z_s,$$
$$\tau_{ij}=\mu\left(u_{i,j}+u_{j,i}-\frac{2}{3}\delta_{ij}u_{m,m}\right),$$
$$q_j=\kappa T_{,j}+\sum_s \rho D_sh_sz_{s,j}.$$

where z_s is the mole number density per unit mass of species s. The H_s and ΔH_{fs} are the enthalpy and the heat of formation per mole of species s, respectively, $h_s \equiv H_s + \Delta H_{fs}$ and R_u is the universal gas constant. The H_c is the chemical source term vector. The $(x_1,x_2,x_3) \equiv (x,y,z)$ and $(\xi_1,\xi_2,\xi_3) \equiv (\xi,\eta,\zeta)$ are Cartesian and curvilinear coordinate systems, respectively, $(\ )_{,i} \equiv \partial(\ )/\partial x_i$, V is the cell volume and n_{ij} is the cell-interface normal vector. The coefficients μ, κ and D_s are the viscosity, thermal conductivity and diffusivity of species s, respectively. The u_i, ρ, p and T are the x_i velocity, the density, the static pressure and the temperature, respectively.

3.2. Parallel computation

The governing equations are discretized by a finite volume method to follow the time-evolution of the combustion field. The convective terms are evaluated using an upwind TVD (Total Variation Diminishing) numerical flux based on Roe's approximate Riemann solver[9,10]. The higher-order flux is constructed extrapolating the characteristics using two types of flux limiters[11]. The accuracy of this flux is third-order in smooth regions and keeps second-order around regions where the sign of characteristics gradient changes. The viscous terms are evaluated with standard second-order difference formulae. The diffusion fluxes at the cell interfaces are modified so that the total mass is conserved[12]. The time integration method is the explicit Runge-Kutta multi-stage method. The second order time integration is used.

The space and time resolution is fine to reproduce the turbulent combustion. The grid spacing is about 50μm, which is about 1/10 of the fuel consumption layer thickness of 1-D hydrogen/air stoichiometric laminar premixed flame calculated by 1-D laminar premixed flame computation code PREMIX[13]. The simulation resolves the fuel consumption layers with about 10 grid points. The time step is about 5nsec, which is much smaller than the chemical reaction time scales. Totally, about 200 million grid points are used for the simulation of $2.5cm^3$ domain.

The parallel computations have been conducted using CeNSS (Central Numerical Simulation System) installed at Japan Aerospace Exploration Agency. Figure 2 illustrates the domain composition and the parallelization method. The main grid system is rectangular and is decomposed into 72 sub-domains. Cylindrical grid system is patched around the injection nozzle and is decomposed into 3 sub-domains. One process is assigned to each sub-domain and the communication between processes is done by MPI. OpenMP technique is used for the intra-process parallelization and several CPUs are assigned to each process. Totally, 291 CPUs are used.

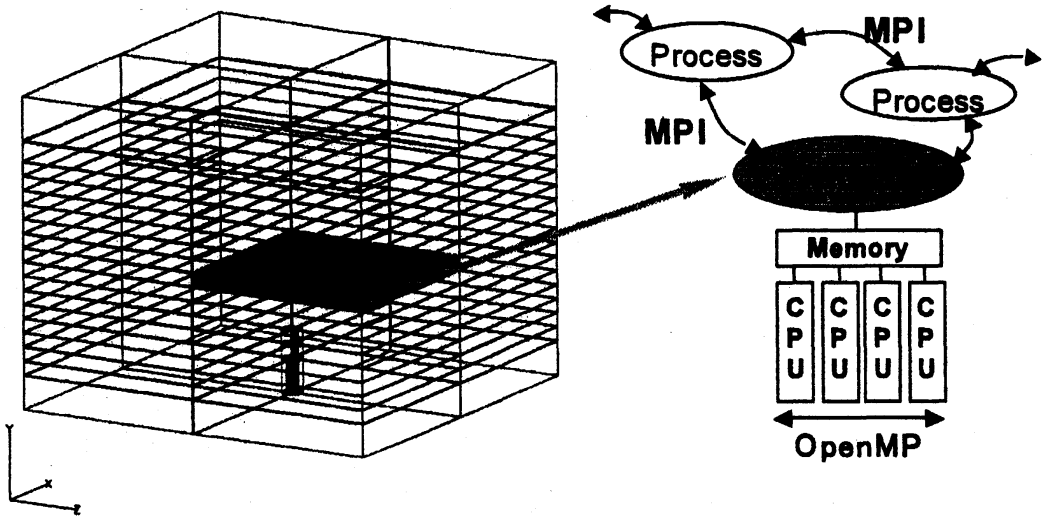

Figure 2: Domain decomposition and parallelization

4. Results and discussion

4.1. Overview of combustion field

The overview of the simulated combustion field is presented in Fig.3. Figure3 a) shows the instantaneous hydrogen jet structure. The iso-surfaces of hydrogen mole fraction at 60% are drawn, where the surface color indicates the surface temperature. The jet flowfied has a strongly 3-D and turbulent features. In the unburnt region, very small structures exist, while in the burnt region, such small structures are not observed. The small structures produced by the Kelvin-Helmholtz (K-H) instability of the unburnt hydrogen jet are suppressed by the increased diffusivity of the burnt hot gas. Figure 3 b) is the iso-surface of temperature at 1000K. The upstream end of the flame transforms and moves up and down in time. The averaged lift-off height is about 6.5D, which shows fairly good agreement with the experimental observation. Figure 3 c) is the Schlieren image made by the post-processing of the 3-D simulation data. Schlieren image, a conventional optical visualization technique, gives the 2-D shadow pattern based on the refractive index gradient that is integraged in the perpendicular direction to the image.

Figure 4 a)-c) present the instantaneous distributions of OH mass-fraction, fuel consumption rate and heat release rate in a 2-D cutting plane. The OH distribution, which is often visualized in recent experimental measurement, shows that the OH distributes along the envelope of the flame, not inside the flame. The remarkable feature understood from the distributions of the fuel consumption rate and heat release rate is that the fuel consumption and heat release take place mainly at the upstream end of the flame and the combustion in downstream is not so strong.

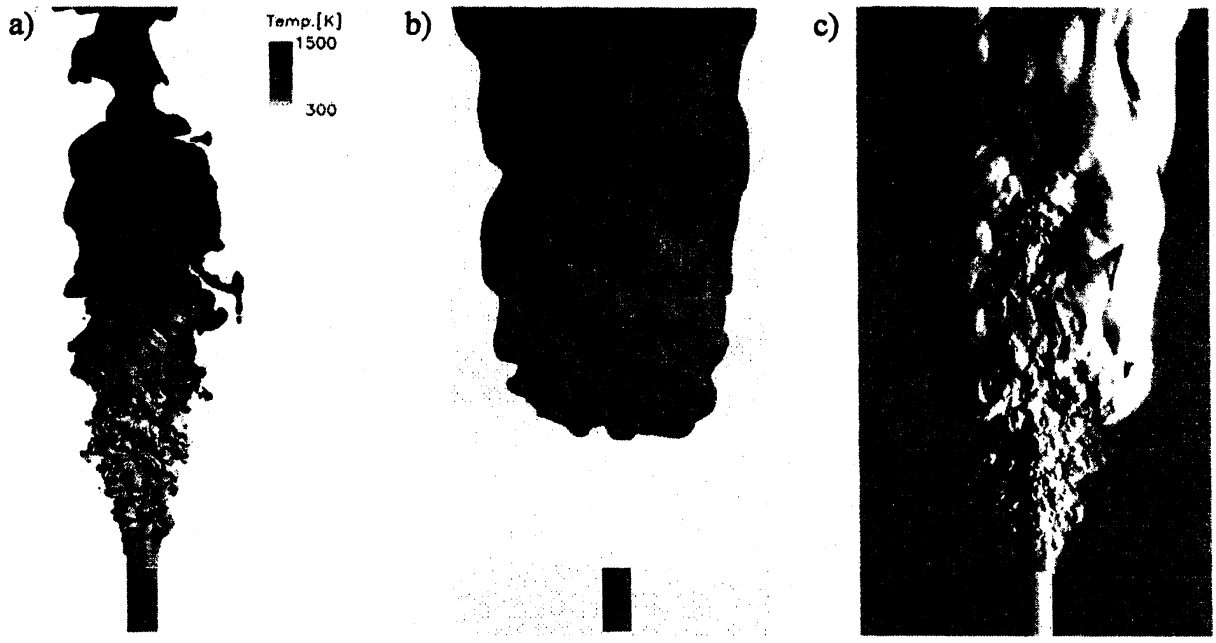

Figure 3: Overview of simulated combustion field. a): Iso-surface of hydrogen mole fraction at 60% with surface color corresponding to the temperature. b): Iso-surface of temperature at 1000K. c): Schlieren image.

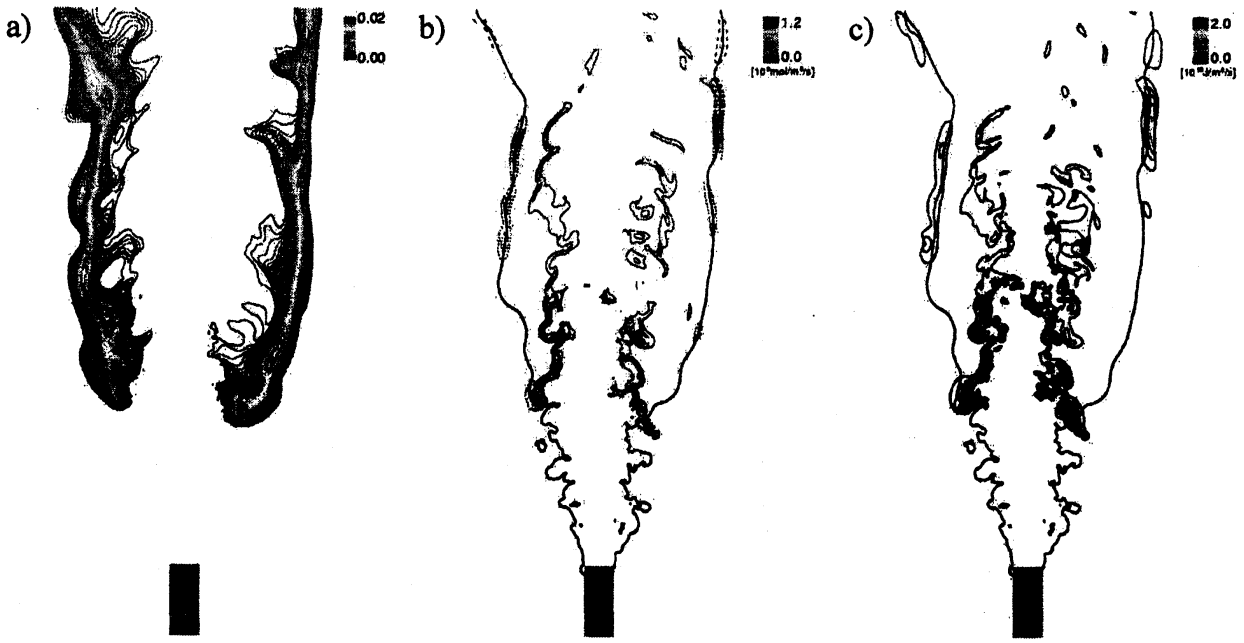

Figure 4: 2-D distributions of a) OH mass fraction, b) fuel consumption rate, c) heat release rate. Thick lines in b) and c) are the stoichiometric lines.

Aforementioned phenomena may be understood by the experimental measurements. The Schlieren image is easily visualized in experiments and even from this 2-D image, we can grasp some aspects of the jet field and flame lift-off height. The optical measurement method has been advancing and the 2-D image in a cutting plane is possible now. The 2-D shapes of OH, fuel consumption and heat release rate distributions can be visualized recenlty by optical measurements based on laser technique. But 3-D or quantitative measurement is not so practical and, therefore, the structure inside the flame envelope cannot be observed. The only means to aquire 3-D quantitative data is 'numerical experiment' at this moment. In the following, the analysis that can be conducted only by numerical experiment will be shown and the obtained new finding will be presented.

4.2. New findings

By analyzing the numerical data, we can reveal the inner combustion phenomena provided that the simulation captures the dominant features of the combustion field. In our studies, the flame structure is analyzed first using the Flame Index [14]. Flame Index (F.I.) is defined as,

$$\text{F.I.} = \nabla Y_{H2} \cdot \nabla Y_{O2} \tag{2}$$

where Y_S denotes the mass fraction of chemical species s.

This index tells the local combustion mode, premixed or diffusive. When this index is positive, the combustion mode is premixed, that is, the combustion surface propagates like a wave, and the fuel and oxidizer diffuse in the same direction from unburnt to burnt side across the combustion surface. When negative, the combustion mode is diffusive, that is, combustion

takes place along the stoichiometric (mixture condition at which fuel and oxidizer burn completely) surface, and the fuel and oxidizer diffuse from the opposite sides toward the stoichiometric surface.

Figure 5 shows instantaneous iso-surfaces of hydrogen consumption rate at 10^4mol/m^3/sec approximately representing the combustion surfaces. The surface color indicates the local combustion mode, black: fuel-lean premixed, white: fuel-rich premixed, gray: diffusive. The modes are identified by Flame Index and the local mixture composition. The figure clearly shows that the lifted flame is not a single flame as expected from Fig.1b) and c). The flame is composed of three flame elements, a leading edge flame at the upstream end of the flame, diffusion flame islands at the outer side, and a turbulent rich premixed flame at the inner side.

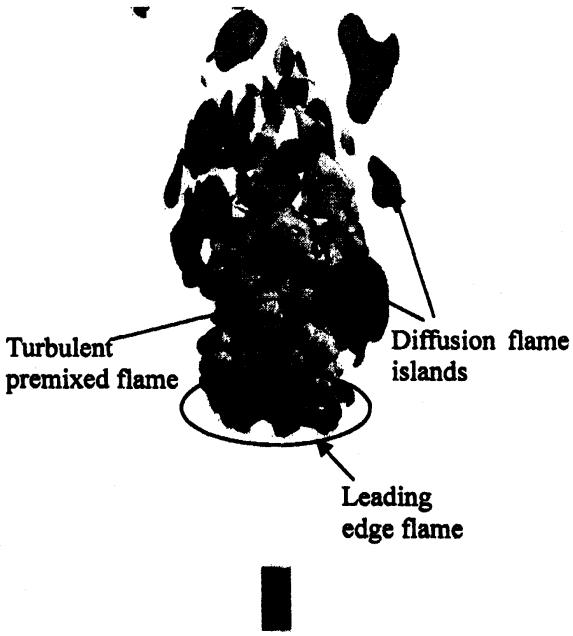

Figure 5: Global flame structure. Iso-surface of fuel consumption rate at 10^4mol/sec/m^3, where surface color indicates combustion mode, white: rich premixed, black: lean premixed, gray: diffusive.

The leading edge flame consists of a diffusion flame in the center, and a lean premixed flame and a rich premixed flame on both sides. Concerning the leading edge flame, the flame stabilization mechanism of a strongly 3-D and unsteady partially premixed flame is the most important issue. The authors have obtained a tentative conclusion that the balance between flame propagation speed and incoming flow speed stabilizes the leading edge flame [1)], but still in progress.

The formation processes of the island-like structure of the outer diffusion flames are investigated and two mechanisms are found [3)]. One takes place in the downstream by the turbulent behavior of the inner rich premixed flame (Fig.6), and the other due to the K-H instability of the unburnt hydrogen jet flow near the leading edge flame.

The inner rich premixed flame shows largely different characteristics from the conventional laminar flame concept. The laminar flame concept, that has been the base of the practical combustion simulation models, assumes the balance between fuel consumption by combustion reactions and fuel supply by molecular diffusion. In the large part of the inner rich premixed flame, the balance does not held and unconventional flame features are observed, for example, the shape of heat release layers are largely deviated from that of fuel consumption layers as shown in Fig.7. Statistical prost-processing shows that the scale of the turbulence eddies are smaller than the reaction layers and they modify the internal structure of the flame [15)]. The analysis based on the conventional laminar flame concept is no longer applicable to this kind of flames, and we need a new concept or new analytical method to

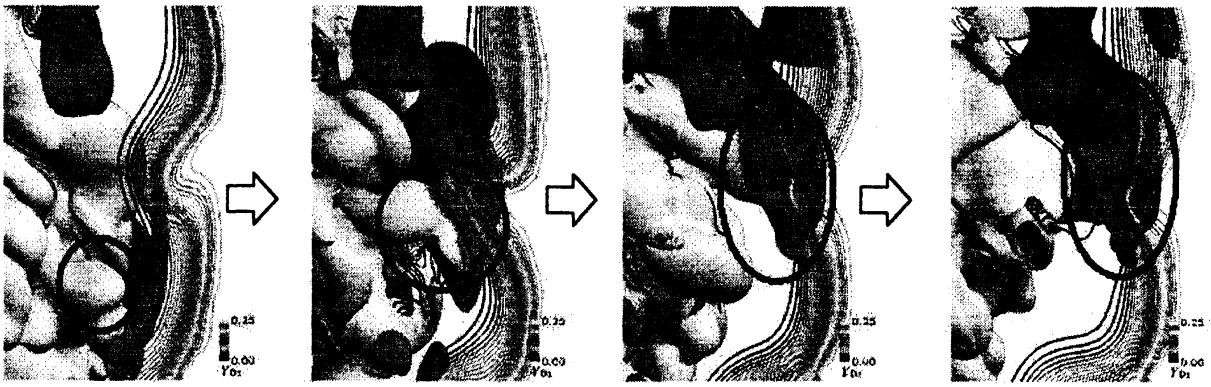

Figure 6: Formation process of diffusion flame island by turbulent behavior of inner rich premixed flame. A diffusion flame island is produced when inner rich premixed flame come in contact with the outer O_2 molecular diffusion layer. Iso-lines are the O_2 mass fraction contours and display the O_2 molecular diffusion layer.

understand and to model this kind of flames.

As described above, on one hand, the simulation reveals interesting properties of laminar flames, and on the other they also have demonstrated very complicated nature of turbulent flame structures. The former findings include time-dependent 3-D structures of partially premixed flames, as well as of conventional premixed and diffusion flames. The latter findings should be very useful to construct combustion models for practical turbulent combustion simulations. We have to develop new methodologies to understand the observed flame behavior and to utilize these findings.

Figure 7: Deviation of heat release layer from fuel consumption layer in inner turbulent rich premixed flame. a): fuel consumption rate distribution, b): heat release rate distribution.

5. Subjects for future studies

This kind of simulations produces enormous amount of data. They contain a lot of information inside. Some can be understood by conventional concepts and principles, but some cannot. The significance of this kind of studies lies in finding the latter phenomena and in developing analytical and computational models to describe the phenomena. To this end, we have to find and develop novel theoretical concepts and analysis principles. This task cannot be completed only by numerical simulation researchers, and the support of analytical scientists, so called 'modeler' is indispensable, for example. Interdisciplinary collaboration will be the key in the future of this kind of studies. Conducting the large scale simulation is not the goal of the research but just the starting point.

As for the computation technique, we should explore higher accuracy of computation. When we like to improve accuracy of a finite volume method, we usually extend stencil to far grid points and then use information at very far grid points. Some methods use information at all the grid points to compute about one grid point. The order of accuracy increases in terms of Taylor expansion in this manner. This approach may be appropriate when we solve incompressible fluid equations, because the sound of speed is infinitely fast and then every grid point is allowed to affect the entire computational domain and vice versa. On the other hand, when we deal with the unsteady compressible flow, the speed of sound is finite, and obviously very far information cannot reach the computation cell during the time integration interval. Hence using very far grid point information does not seem a sound means to improve the quality of the unsteady compressible flow simulations, while it may be sound for steady problems. The clear guideline and criteria about the stencil extension range (distance and direction) are needed to improve the quality of compressible unsteady simulation in a sound way.

6. Summary

Large-scale detailed simulation is a very useful means to understand the physics and chemistry of complicated combustion phenomena. It provides us with novel and valuable information that cannot be obtained from conventional flame theories or experimental measurements. However, we have to develop novel methodologies of analysis to bring its potential into full play.

Acknowledgements

This research was carried out as a research activity at the Center for Smart Control of Turbulence funded by MEXT (Ministry of Education, Culture, Sports, Science and Technology) of Japan.

Table 1: Chemical Kinetics

$$k = AT^n \exp(-E_a/RT)$$

	Reaction	Forward rate			Reverse rate		
		$\log A$	n	E_a	$\log A$	n	E_a
1	$H + O_2 \rightleftharpoons O + OH$	14.27	0	16.79	13.17	0	0.68
2	$H_2 + O \rightleftharpoons H + OH$	10.26	1	8.90	9.92	1	6.95
3	$H_2O + O \rightleftharpoons OH + OH$	13.53	0	18.35	12.50	0	1.10
4	$H_2O + H \rightleftharpoons H_2 + OH$	13.98	0	20.30	13.34	0	5.15
5	$H_2O_2 + OH \rightleftharpoons H_2O + HO_2$	13.00	0	1.80	13.45	0	32.79
6	$H_2O + M \rightleftharpoons H + OH + M$	16.34	0	105.00	23.15	−2	0.00
7	$H + O_2 + M \rightleftharpoons HO_2 + M$	15.22	0	−1.00	15.36	0	45.90
8	$HO_2 + O \rightleftharpoons OH + O_2$	13.70	0	1.00	13.81	0	56.61
9	$HO_2 + H \rightleftharpoons OH + OH$	14.40	0	1.90	13.08	0	40.10
10	$HO_2 + H \rightleftharpoons H_2 + O_2$	13.40	0	0.70	13.74	0	57.80
11	$HO_2 + OH \rightleftharpoons H_2O + O_2$	13.70	0	1.00	14.80	0	73.86
12	$H_2O_2 + O_2 \rightleftharpoons HO_2 + HO_2$	13.60	0	42.64	13.00	0	1.00
13	$H_2O_2 + M \rightleftharpoons OH + OH + M$	17.08	0	45.50	14.96	0	−5.07
14	$H_2O_2 + H \rightleftharpoons HO_2 + H_2$	12.23	0	3.75	11.86	0	18.70
15	$O + H + M \rightleftharpoons OH + M$	16.00	0	0.00	19.90	−1	103.72
16	$O_2 + M \rightleftharpoons O + O + M$	15.71	0	115.00	15.67	−0.28	0.00
17	$H_2 + M \rightleftharpoons H + H + M$	14.34	0	96.00	15.48	0	0.00

References

1) Mizobuchi, Y., Tachibana, S., Shinjo, J., Ogawa, S., and Takeno, T., Proc. Combust. Inst. 29, 2002, pp. 2009-2015.

2) Westbrook, C. K., Mizobuchi, Y., Poinsot, T. J., Smith, P. J. and Warnatz, J., Proc. Combust. Inst. 30, 2004, pp. 125-157.

3) Mizobuchi, Y., Shinjo, J., Ogawa, S. and Takeno, T., Proc. Combust. Inst. 30, 2004, pp. 611-619.

4) Cheng, T. S., Wehrmeyer, J. A. and Pitz, R. W., Combustion and Flame, 91, 1992, pp. 323-345.

5) Westbrook,C.K. Combustion Science and Technology, 29, 1982, pp.67-81.

6) Chapman, S., and Cowling, T.G., *The Mathematical Theory of Non-Uniform Gases*, Cambridge University Press, 1970.

7) Wilke, C. R., *J. Chem. Phys.*, 18(4):517-519 (1950).

8) *JANAF Thermo-chemical Tables,* Clearinghouse for Federal Scientific and Technical Information, Washington, DC, 1965.

9) Roe,P.L., Journal of Computational Physics, 43:357-372, 1981.

10) Wada,Y., Ogawa,S. and Ishiguro,T., AIAA paper 89-0202, 1989.

11) Wada,Y., *Numerical Simulation of High-Temperature Gas Flows by Diagonalization of Gasdynamic Matrices*, PhD thesis, the University of Tokyo, 1995.

12) Mizobuchi,Y. and Ogawa,S., AIAA paper 2000-0184, 2000.

13) Kee, R. J. et al, Sandia report sand 85-8240(1985), Sandia National Laboratory

14) Yamashita, H., Shimada, M. and Takeno, T., Twenty-sixth Symposium (International) on Combustion, The Combustion Institute, Pittsburgh, 1996, pp. 27-34.

15) Takeno, T. and Mizobuchi, Y., Comptes Rendus Mechanique, 334, 2006, pp.517-522.